

# Chiral Invariant Phase Space Event Generator

## III. Modeling of real and virtual photon interactions with nuclei below pion production threshold.

P.V. Degtyarenko<sup>1</sup>, M.V. Kossov<sup>2</sup>, and H.-P. Wellisch<sup>3</sup>

<sup>1</sup> Thomas Jefferson National Accelerator Facility, Newport News, Virginia, USA

<sup>2</sup> Institute of Theoretical and Experimental Physics, Moscow, Russia

<sup>3</sup> CERN, 1211 Geneva, Switzerland

Received: date / Revised version: date

**Abstract.** Nuclear fragment production in photonuclear reactions below pion production threshold is implemented in the developed version of the new event generator, based on the CHIPS model, within the GEANT4 simulation toolkit. The spectra of secondary nucleons in the photonuclear process are compared with experimental data.

**PACS.** 02.70.Lq Monte Carlo and statistical methods – 12.38.Mh Quark gluon plasma – 21.60.Ka Monte Carlo models in nuclear structure – 24.10.Lx Monte Carlo simulations (including hadron and parton cascades and string breaking models) in nuclear reactions: general – 24.85.+p Quarks, gluons, and QCD in nuclei and nuclear processes

## 1 Introduction

In previous publications [1], [2] we applied the CHIPS model of hadronic and nuclear fragmentation to antiproton-proton annihilation and pion capture by nuclei at rest. It was not necessary to consider the angular dependences in these reactions. The projectile particle was considered to be captured by a nuclear cluster in the nucleus, thus creat-

ing a Quasmon which then distributes its energy isotropically. In the example of the photonuclear reaction discussed in Ref. [2], namely the description of 90° proton and deuteron spectra in  $A(\gamma, X)$  reactions at  $E_\gamma = 59-65$  MeV, the assumption on the initial Quasmon excitation mechanism was the same. The description of the 90° data was satisfactory, but the generated data showed very lit-

tle angular dependence, as the velocity of Quasmons produced in the initial state was small, and the fragmentation process was almost isotropic. Experimentally, the angular dependence of secondary protons in photo-nuclear reactions is quite strong even at low energies (see, for example, Ref. [3]). This is a challenging experimental fact which is difficult to explain in any model. It's enough to say that if the angular dependence of secondary protons in the  $\gamma^{40}\text{Ca}$  interaction at 60 MeV is analyzed in terms of relativistic boost, then the velocity of the source should reach  $0.33c$ ; hence the mass of the source should be less than pion mass. The main subject of the present publication is to show that the quark-exchange mechanism used in the CHIPS model can not only model the clusterization of nucleons in nuclei and hadronization of intranuclear excitations into nuclear fragments, but can also model complicated mechanisms of interaction of photons and hadrons in nuclear matter.

## 2 Photon absorption model

In Ref. [2] we defined a quark-exchange diagram which helps to keep track of the kinematics of the quark-exchange process (see Fig. 1 in Ref. [2]). To apply the same diagram to the first interaction of a photon with a nucleus, it is necessary to assume that the quark-exchange process takes place in nuclei continuously, even without any external interaction. Nucleons with high momenta do not leave the nucleus because of the lack of excess energy. The hypothesis of the CHIPS model is that the quark-exchange forces between nucleons [4] continuously create clusters in normal nuclei. Since a low-energy photon (below the pion

production threshold) cannot be absorbed by a free nucleon, other absorption mechanisms involving more than one nucleon have to be used.

The simplest scenario is photon absorption by a quark-parton in the nucleon. At low energies and in vacuum this does not work because there is no corresponding excited baryonic state. But in nuclear matter there is a possibility to exchange this quark with a neighboring nucleon or a nuclear cluster. The diagram for the process is shown in Fig. 1. In this case the photon is absorbed by a quark-parton from the parent cluster  $\text{PC}_1$ , and then the secondary nucleon or cluster  $\text{PC}_2$  absorbs the entire momentum of the quark and photon. The exchange quark-parton  $q$  restores the balance of color, producing the final-state hadron  $F$  and the residual Quasmon  $\text{RQ}$ . The process looks like a knockout of a quasi-free nucleon or cluster out of the nucleus. It should be emphasized that in this scenario the CHIPS event generator produces not only “quasi-free” nucleons but “quasi-free” fragments too. The yield of these quasi-free nucleons or fragments is concentrated in the forward direction.

The second scenario which provides for an angular dependence is the absorption of the photon by a colored fragment ( $\text{CF}_2$  in Fig. 2). In this scenario, both the primary quark-parton with momentum  $k$  and the photon with momentum  $q_\gamma$  are absorbed by a parent cluster ( $\text{PC}_2$  in Fig. 2), and the recoil quark-parton with momentum  $q$  cannot fully compensate the momentum  $k + q_\gamma$ . As a result the radiation of the secondary fragment in the forward direction becomes more probable.

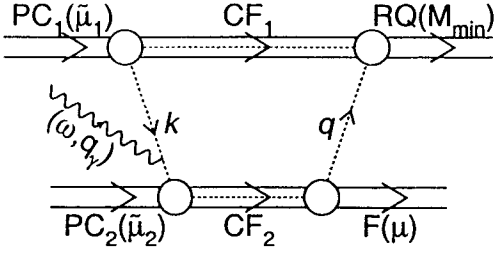


Fig. 1. Diagram of photon absorption in the quark exchange mechanism.  $PC_{1,2}$  stand for parent clusters with bound masses  $\bar{\mu}_{1,2}$ , participating in the quark-exchange.  $CF_{1,2}$  stand for the colored nuclear fragments in the process of quark exchange.  $F(\mu)$  denotes the outgoing hadron with mass  $\mu$  in the final state.  $RQ$  is the residual Quasmon which carries the rest of the excitation energy and momentum.  $M_{min}$  characterizes its minimum mass defined by its quark content. Dashed lines indicate colored objects. The photon is absorbed by a quark-parton  $k$  from the parent cluster  $PC_1$ .

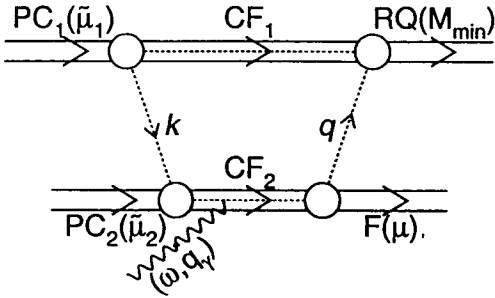


Fig. 2. Diagram of photon absorption in the quark-exchange mechanism. The notation is the same as in Fig. 1. The photon is absorbed by the colored fragment  $CF_2$ .

In both cases the angular dependence is defined by the first act of hadronization. The further fragmentation of the residual Quasmon is almost isotropic.

### 3 Algorithm of the first $\gamma A$ interaction calculation

It was shown in [1] that the energy spectrum of quark partons in a Quasmon can be calculated as

$$\frac{dW}{k^* dk^*} \propto \left(1 - \frac{2k^*}{M}\right)^{N-3}, \quad (1)$$

where  $k^*$  is the energy of the primary quark-parton in the Center of Mass System (CMS) of the Quasmon,  $M$  is the mass of the Quasmon, and  $N$ , the number of quark-partons in the Quasmon, can be calculated from the equation

$$\langle M^2 \rangle = 4 \cdot N \cdot (N - 1) \cdot T^2. \quad (2)$$

Here  $T$  is the temperature of the system.

In the first scenario of the  $\gamma A$  interaction (Fig. 1), as both interacting particles are massless, we assumed that the cross section for the interaction of the photon with a particular quark-parton is proportional to the charge of the quark-parton squared, and inversely proportional to the mass of the photon-parton system  $s$ , which can be calculated as

$$s = 2\omega k(1 - \cos(\theta_k)). \quad (3)$$

Here  $\omega$  is the energy of the photon, and  $k$  is the energy of the quark-parton in the Laboratory System (LS):

$$k = k^* \cdot \frac{E_N + p_N \cdot \cos(\theta_k)}{M_N}. \quad (4)$$

In the case of a virtual photon, equation (3) can be written as

$$s = 2k(\omega - q_\gamma \cdot \cos(\theta_k)), \quad (5)$$

where  $q_\gamma$  is the momentum of the virtual photon. In both cases equation (1) transforms into

$$\frac{dW}{dk^*} \propto \left(1 - \frac{2k^*}{M}\right)^{N-3}, \quad (6)$$

and the angular distribution in  $\cos(\theta_k)$  converges to a  $\delta$ -function: in the case of a real photon  $\cos(\theta_k) = 1$ , and in the case of a virtual photon  $\cos(\theta_k) = \frac{\omega}{q_\gamma}$ .

In the second scenario for the photon interaction (Fig. 2) we assumed that both the photon and the primary quark-parton, randomized according to equation (1), enter the parent cluster  $PC_2$ , and after that the normal procedure of quark exchange continues, in which the recoiling quark-parton  $q$  returns to the first cluster.

An additional parameter in the model is the relative contribution of both mechanisms. As a first approximation we assumed equal probability, but in the future, when more detailed data are obtained, this parameter can be adjusted.

## 4 Comparison with data

We begin the comparison with the data on proton production in the  $^{40}\text{Ca}(\gamma, X)$  reaction at  $90^\circ$  at 59–65 MeV [5], and at  $60^\circ$  and  $150^\circ$  at 60 MeV [7]. We analyzed these data together to compare the angular dependence generated by CHIPS with experimental data. The data are presented as a function of the invariant inclusive cross section  $f = \frac{d\sigma}{p_p dE_p}$  depending on the variable  $k = \frac{T_p + p_p}{2}$ , where  $T_p$  and  $p_p$  are the kinetic energy and the momentum of the secondary proton. As one can see from Fig. 3, the angular dependence of the proton yield in photoproduction on

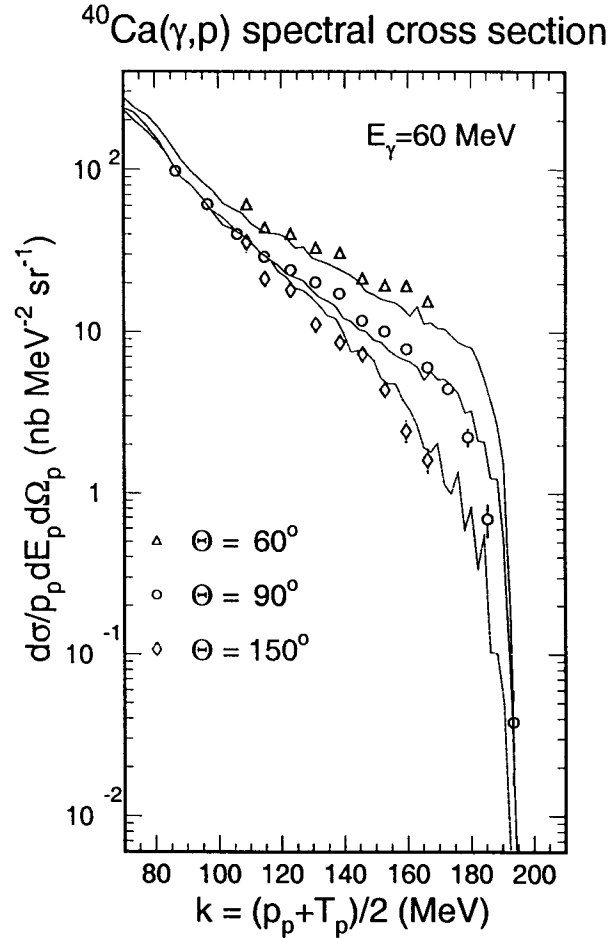


**Fig. 3.** Comparison of the CHIPS model results (lines in the figure) with the experimental data [5] on proton spectra at  $90^\circ$  in the photonuclear reactions on  $^{40}\text{Ca}$  at 59–65 MeV (open circles), and proton spectra at  $60^\circ$  (triangles) and  $150^\circ$  (diamonds). Statistical errors in the CHIPS results are not shown but can be judged by the point-to-point variations in the lines. The comparison is absolute, using the value of total photonuclear cross section of 5.4 mb for Ca, as given in Ref. [6].

$^{40}\text{Ca}$  at 60 MeV is reproduced quite well by the CHIPS event generator.

The second set of measurements that we use for the benchmark comparison deals with the secondary proton

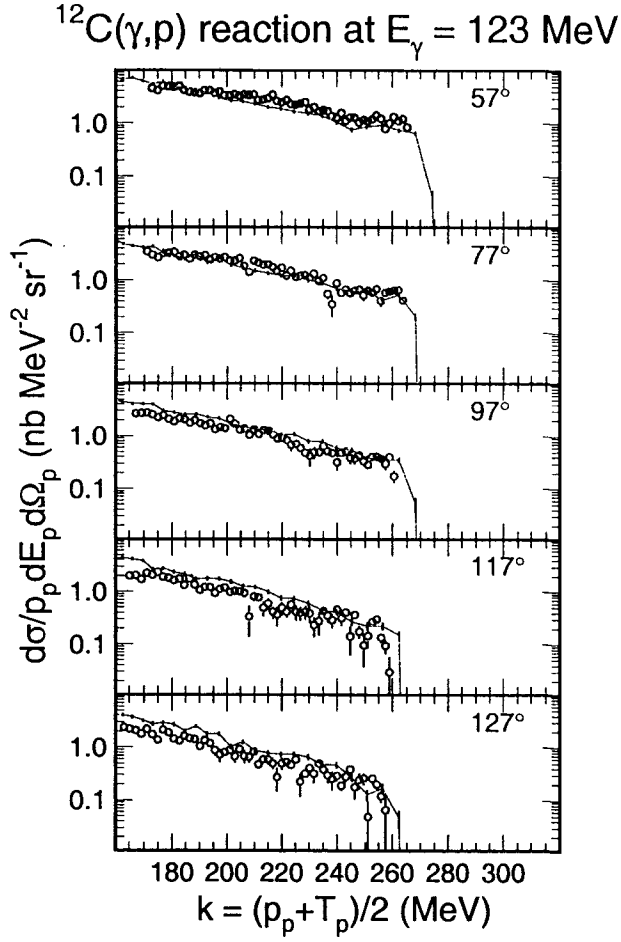


Fig. 4. Comparison of the CHIPS model results (lines in the figure) with the experimental data [8] on proton spectra at  $57^\circ$ ,  $77^\circ$ ,  $97^\circ$ ,  $117^\circ$ , and  $127^\circ$  in the photonuclear reactions on  $^{12}\text{C}$  at 123 MeV (open circles). The value of the total photonuclear cross section was set at 1.8 mb.

yields in  $^{12}\text{C}(\gamma, X)$  reactions at 123 and 151 MeV [8], which is still below the pion production threshold on a free nucleon. Inclusive spectra of protons have been measured in  $\gamma^{12}\text{C}$  reactions at  $57^\circ$ ,  $77^\circ$ ,  $97^\circ$ ,  $117^\circ$ , and  $127^\circ$ . Originally, these data were presented as a function of the missing energy. We present the data in Figs. 4 and 5 together with CHIPS calculations in the form of the invari-

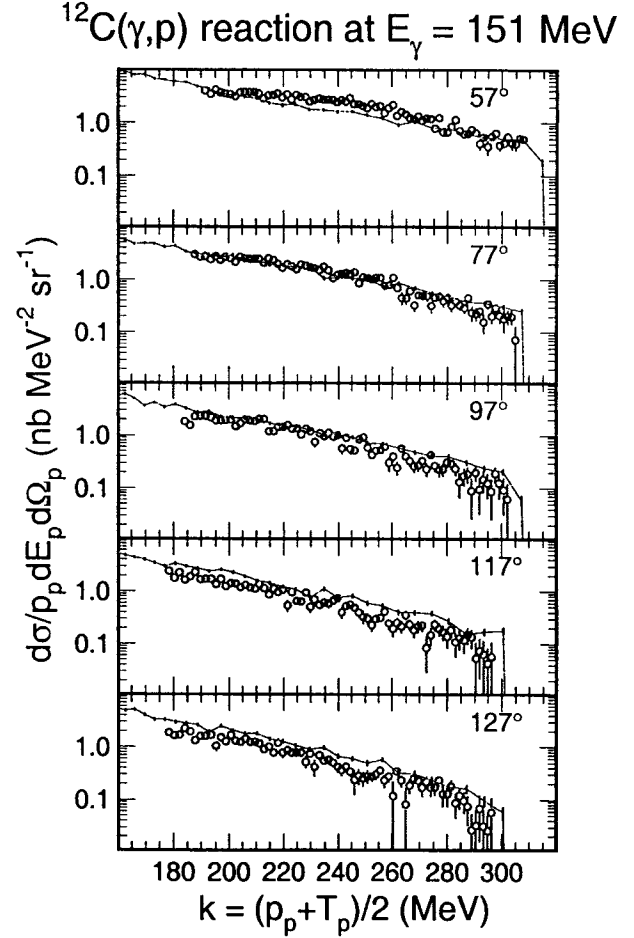


Fig. 5. Same as in Fig. 4, for the photon energy 151 MeV.

ant inclusive cross section dependent on  $k$ . All parameters of the model such as temperature  $T$  and parameters of clusterization for the particular nucleus were the same as in Ref. [2], where pion capture spectra were fitted. The agreement between the experimental data and the CHIPS model results is quite remarkable. Both data and calculations show significant strength in the proton yield cross section up to the kinematical limits of the reaction. The angular distribution in the model is not as prominent as in the experimental data, but agrees well qualitatively.

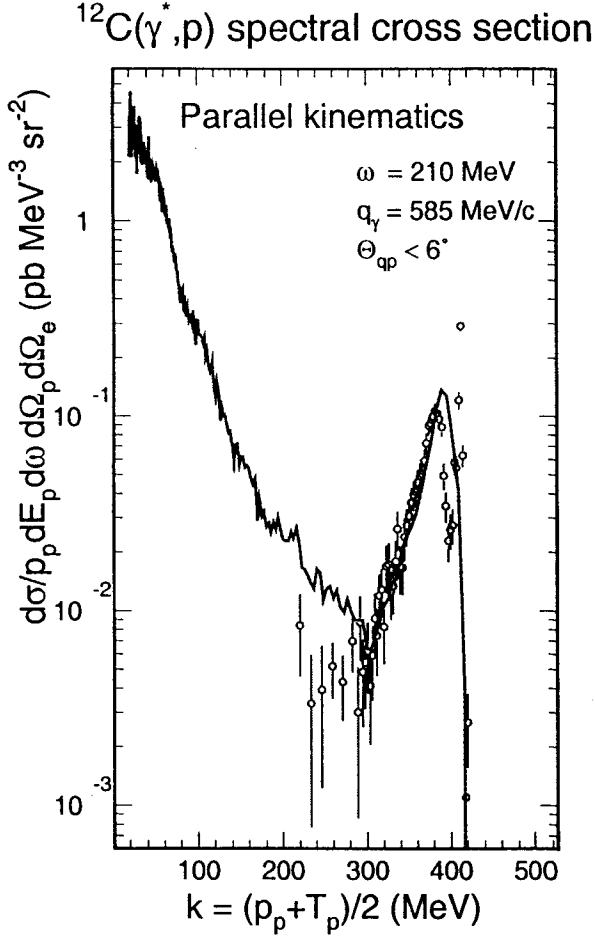


Fig. 6. Comparison of the CHIPS model results (line in the figure) with the experimental data [9] (open circles) on the proton spectrum measured in parallel kinematics in the  $^{12}\text{C}(e, e'p)$  reaction at an energy transfer equal to 210 MeV and momentum transfer equal to 585 MeV/c. Statistical errors in the CHIPS result are not shown but can be judged by the point-to-point variations in the line. The relative normalization is arbitrary.

Using the same parameters, we applied the CHIPS event generator to the  $^{12}\text{C}(e, e'p)$  reaction measured in Ref.[9]. The proton spectra were measured in parallel kinematics in the interaction of virtual photons with energy  $\omega = 210$  MeV and momentum  $q_\gamma = 585$  MeV/c. To ac-

count for the experimental conditions in the CHIPS event generator, we have selected protons generated in the forward direction with respect to the direction of the virtual photon, with the relative angle  $\Theta_{qp} < 6^\circ$ . The CHIPS generated distribution and the experimental data are shown in Fig. 6 in the form of the invariant inclusive cross section as a function of  $k$ . The CHIPS event generator works only with ground states of nuclei so we did not expect any narrow peaks for  $^1p_{3/2}$ -shell knockout or for other shells. Nevertheless we found that the CHIPS event generator fills in the so-called “ $^1s_{1/2}$ -shell knockout” region, which is usually artificially smeared by a Lorentzian [10]. In the regular fragmentation scenario the spectrum of protons below  $k = 300$  MeV is normal; it falls down to the kinematic limit. The additional yield at  $k > 300$  MeV is a reflection of the specific first act of hadronization with the quark exchange kinematics. The slope increase with momentum is approximated well by the model, but it is obvious that the yield close to the kinematic limit of the  $2 \rightarrow 2$  reaction can only be described in detail if the excited states of the residual nucleus are taken into account.

## 5 Conclusion

The angular dependence of the proton yield in low-energy photo-nuclear reactions is described in the CHIPS model and event generator. The most important assumption in the description is the hypothesis of a direct interaction of the photon with an asymptotically free quark in the nucleus, even at low energies. This means that asymptotic freedom of QCD and dispersion sum rules [11] can in some

way be generalized for low energies. The knockout of a proton from a nuclear shell or the homogeneous distributions of nuclear evaporation cannot explain significant angular dependences at low energies.

The same mechanism appears to be capable of modeling proton yields in such reactions as the  $^{16}\text{C}(e,e'p)$  reaction measured at MIT Bates [9], where it was shown that the region of missing energy above 50 MeV reflects “two-or-more-particle knockout” (or the “continuum” in terms of the shell model). The CHIPS model may help to understand and model such phenomena.

## Acknowledgment

The work was supported by the U.S. Department of Energy under contract number DE-AC05-84ER4015.

## References

1. P.V. Degtyarenko, M.V. Kossov, H.-P. Wellisch, to be published.
2. P.V. Degtyarenko, M.V. Kossov, H.-P. Wellisch, to be published.
3. Jan Ryckebusch et al., Phys. Rev. C **49** (1994) 2704.
4. K. Maltman and N. Isgur, Phys. Rev. D **29** (1984) 952.
5. D. Ryckbosch et al., Phys. Rev. C **42** (1990) 444.
6. J. Ahrens et al., Nucl. Phys. **A446** (1985) 229c.
7. C. Van den Abeele; private communication cited in the reference: Jan Ryckebusch et al., Phys. Rev. C **49** (1994) 2704.
8. P.D. Harty et al. (unpublished); private communication cited in the reference: Jan Ryckebusch et al., Phys. Rev. C **49** (1994) 2704.
9. L.B. Weinstein et al., Phys. Rev. Lett. **64** (1990) 1646.
10. J.P. Jeukenne and C. Mahaux, Nucl. Phys. A **394** (1983) 445.
11. C. Bernard, A. Duncan, J. LoSecco, and S. Weinberg, Phys. Rev. D **12** (1975) 792; E. Poggio, H. Quinn, and S. Weinberg, Phys. Rev. D **13** (1976) 1958.